SEQUENTIAL INVERSIONS OF SURFACE-WAVE PHASE VELOCITY AND THE FULL WAVEFORM FOR SHALLOW SEISMIC IMAGING

Y. Pan, L. Gao, and T. Bohlen

email: *yudi.pan@kit.edu*
keywords: *MASW, FWI, shallow seismic*

ABSTRACT

Surface waves are widely used in determining near-surface structures. By inverting dispersion curves to obtain local 1D S-wave velocity profiles, multichannel analysis of surface waves (MASW) has been proven as an efficient way to analyze shallow-seismic surface waves. Besides, full-waveform inversion (FWI) also provides a feasible way in reconstructing near-surface structure. The individual adoption of MASW and FWI suffers from relatively low lateral resolution and high ambiguity, respectively. We propose to adopt a sequential MASW and FWI strategy for high-resolution imaging of near-surface structures. A synthetic case study was performed to compare the shapes of objective functions of MASW, FWI, and a modified FWI method. It suggests that a sequential adoption of MASW, modified FWI, and FWI provides an efficient way to delineate near-surface structures. We applied our method to a field data set collected in Olathe, USA. The shape of the bedrock is clearly delineated in the inversion result, which nicely agrees with borehole measurements. It proves that the sequential application of MASW and FWI provides an effective way for high-resolution imaging of near-surface media.

INTRODUCTION

The reconstruction of near-surface elastic-parameter models is of fundamental importance for near-surface geophysical and geotechnical studies. Surface waves dominate the shallow-seismic wavefield, and they are attractive for determining near-surface structures due to their relatively high signal-to-noise ratio in the field recordings. Multichannel analysis of surface waves (MASW) is widely used in estimating near-surface S-wave velocity by analyzing shallow-seismic surface waves. Two main steps in MASW are the measuring and inverting of surface-wave phase velocity (dispersion curve). Based on phase-velocity inversion, MASW assumes a 1D approximation of subsurface structures and allows the reconstruction of S-wave velocity as a function of depth.

With the rapid increase of computational power, it has become feasible to perform full-waveform inversion (FWI) on shallow-seismic wavefields to delineate near-surface structures. Romdhane et al. (2011) have shown the promising prospects of performing FWI on shallow-seismic Rayleigh waves by means of synthetic examples. Pérez Solano et al. (2014) proposed a windowed-amplitude waveform inversion method to invert shallow-seismic surface waves. Köhn et al. (2016) applied time-domain FWI to laboratory ultrasonic Rayleigh waves. Pan et al. (2016) proposed a time-domain Love-wave FWI algorithm and applied it to a field data set. Wittkamp and Bohlen (2016) proved the advantages of performing sequential and joint inversion of different shallow-seismic wavetypes. Groos et al. (2017) showed the high resolution of multi-scale FWI for characterizing near-surface heterogeneity. Nuber et al. (2017) studied the optimization of the geometry of field measurements for shallow-seismic FWI.

In this paper, we propose to use MASW and FWI sequentially to delineate near-surface structures. We illustrate the main steps in MASW and FWI, and some modified FWI strategies. A synthetic model is used

to study the stability and resolution of MASW and FWI-based methods. Then, we apply the sequential-inversion method to a field data set collected in Olathe, USA, for bedrock mapping. The inversion result is compared to borehole data, to verify the validity of the sequential-inversion strategy.

SYNTHETIC EXAMPLE

A two-layer model (Table 1) is used to compare the shapes of MASW and FWI objective functions. The observed and synthetic data for MASW are the fundamental-mode dispersion curves from 10 to 80 Hz with an interval of 2 Hz. The observed and synthetic waveforms for FWI are simulated by finite-difference modelling. A 25 Hz Ricker wavelet is used as source-time function, and is generated vertically. Forty-eight two-component receivers are placed with a nearest offset of 4 m and a trace interval of 1 m, recording both vertical and horizontal components.

Because surface waves are much more sensitive to S-wave velocity than P-wave velocity and density (Groos et al., 2017), we only change the S-wave velocity to test the objective functions. The S-wave velocity model (Vs) depends on two parameters: a top-layer velocity Vs_top and a homogeneous half-space (bedrock) velocity Vs_bedrock. Several Vs models are tested with Vs_top and Vs_bedrock ranging from 100 to 300 m/s and 300 to 500 m/s, respectively. The P-wave velocity and density models are kept the same as the true model (Table 1) for all synthetic models.

	S-wave velocity (m/s)	P-wave velocity (m/s)	density (g/cm^3)	thickness (m)
Layer 1	200	500	2.0	5
Layer 2	400	1000	2.0	∞

Table 1: A two-layer synthetic model.

The shapes of the objective functions of all FWI tests, including classical FWI, MFWI (M: multiscale, with a high-cut filter of 10 Hz), AFWI (A: amplitude) and EFWI (E: envelope) are shown in Figure 1. The global minimum (area in blue color in Figure 1) is quite narrow in the case of FWI, and is broader in MFWI, AFWI and EFWI. Most of the gradients in the objective functions are heading along the Vs_bedrock axis, indicating that FWI methods are more sensitive to the bedrock (background) velocity compared to that of the top layer. In the objective function of FWI, almost all its gradients head towards wrong directions when the bedrock velocity is more than 5% off its true value (Vs_bedrock $>$ 420 m/s or Vs_bedrock $<$ 380 m/s). It shows the large degree of dependence of FWI on the initial model (bedrock-velocity of the initial model should be less than 5% off its true value to ensure the convergence of the inversion). The dependence on the initial model is mitigated in MFWI, AFWI, and EFWI. Around 67, 75 and 99 percent of the gradients in MFWI, AFWI, EFWI objective functions, respectively, are heading towards the correct bedrock velocity. The EFWI has the widest global minimum region and least nonlinearity among all the FWI-based objective functions.

Similarly, we calculate the MASW objective function (Figure 2). The MASW objective function shows a wide global minimum, which is at least 8, 4 and 2 times wider than that of FWI, AFWI and EFWI, respectively. All the gradients in the MASW objective function (arrows in Figure 2) point towards the correct bedrock velocity, indicating a low dependence of MASW on the initial model. Because the computational time of MASW is much lower than for the FWI-based methods, it is always worth to perform MASW prior to FWI. The choice of the modified FWI to use should be target-oriented. In the following case in which we aim at mapping bedrock, we adopt a sequential use of MASW, MFWI and then FWI. This is because the bedrock mainly influences the low-frequency (long-wavelength) component of surface waves, so that we can enhance the sensitivity of FWI to the bedrock by manually performing more iterations in low-frequency ranges in MFWI.

FIELD EXAMPLE

A set of field data was collected at Olathe, USA. Vertical source and forty-five vertical-component geophones were placed along the survey line, with a nearest offset of 3.6 m and a trace interval of 0.6 m. A roll-along manner was used during data acquisition, and the whole spread was moved 1.2 m (2 traces)

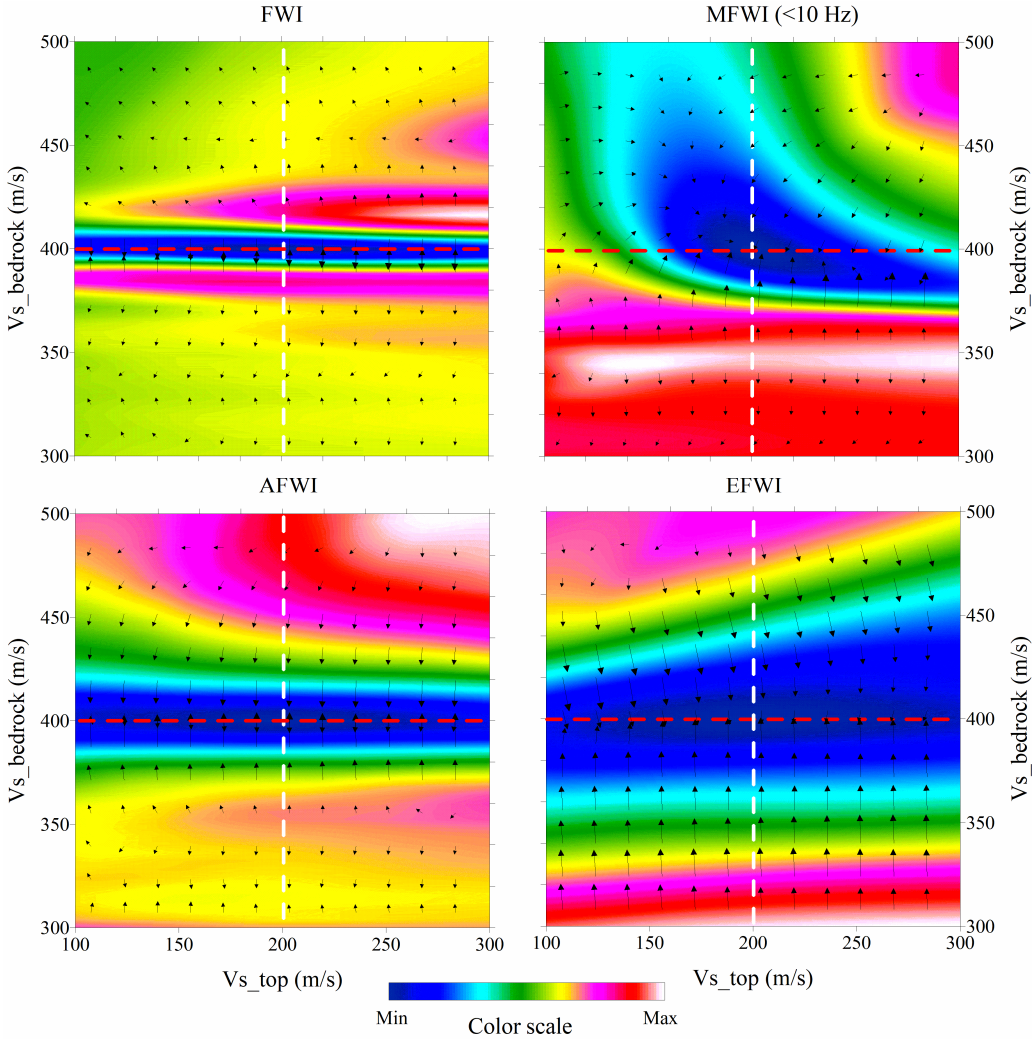

Figure 1: Objective functions for FWI methods. Arrows represent gradient directions of the obj. function.

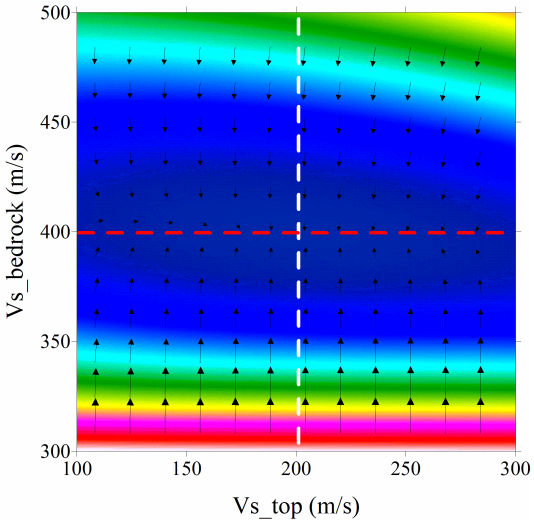

Figure 2: Objective function for MASW. Arrows represent gradient directions of the objective function.

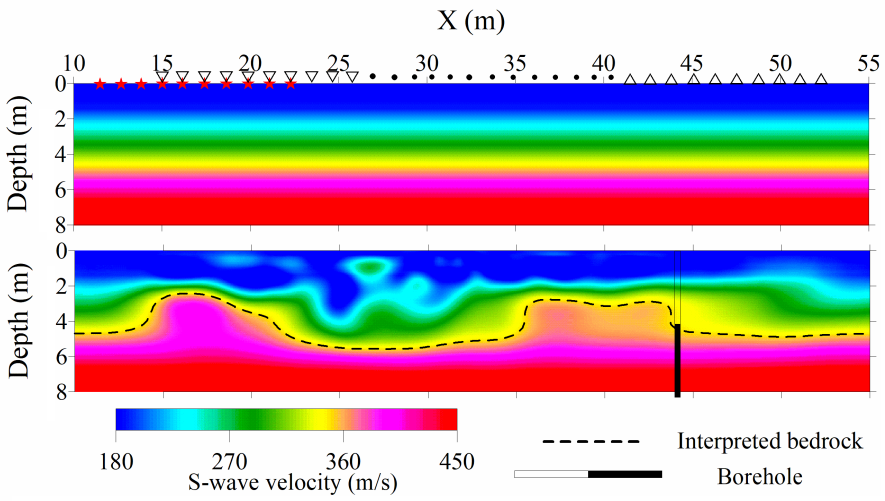

Figure 3: S-wave velocity model of the inversion result. Stars represent the locations of ten sources. Pairs of inversed and upright triangles represent the locations of the first and last traces, respectively, in each shot gather.

towards the eastern direction (end of spread) with each new shot. A total of ten shot gathers are used in this paper.

We used MASW to build an initial model for FWI (upper image in Figure 3). Before the waveform inversion, we applied a 3D to 2D transformation to the observed data to remove the phase shift caused by the 2D forward solver (Forbriger et al., 2014). We started MFWI by inverting a subset of data up to 35 Hz. The upper frequency limit of the low-pass filter is sequentially increased to 45, 60, 80 and 100 Hz. The shortest corresponding wavelengths for those frequencies are 7.2, 4.2, 3.0, 2.2 and 1.8 m, respectively. A conjugate gradient algorithm was adopted as optimization algorithm. A minimum of 11 iterations were performed at each stage, while the inversion moved to the next stage once the improvement in the misfit value became less than 1%. The misfit function converged after 62 iterations.

The inversion result clearly shows the shape of bedrock (dashed line in Figure 3). The bedrock ranges from 2 to 6 m in depth, which agrees with borehole data. Besides the shape of the bedrock, the result also shows the lateral change of the thickness of the top layer. A borehole drilled along our survey line shows that the bedrock at that position is 4.2 m deep, which nicely agrees with our inversion result (Figure 3). It proves a relatively high reliability and accuracy of the inversion result obtained by our proposed method.

CONCLUSIONS

We proposed to sequentially use multichannel analysis of surface wave (MASW) and full-waveform inversion (FWI) of surface waves to delineate near-surface structures. A synthetic example was performed to compare shapes of objective functions of MASW, FWI and some modified FWI methods. It shows that MASW possesses high stability but relatively low resolution in imaging near-surface structures, while FWI behaves just the other way around. It suggests that a sequential MASW and FWI strategy can benefit the high-resolution imaging of near-surface structures. We performed this sequential strategy on a real-world data set acquired in Olathe, USA. The sequential-inversion result nicely agrees with available borehole data, indicating relatively high reliability of the result. This study shows that the sequential application of MASW and FWI can provide an effective way for high-resolution imaging of near-surface structures.

ACKNOWLEDGMENTS

The authors would like to thank Prof. Jianghai Xia for providing the real-world data and for fruitful discussion. This work was kindly supported by the sponsors of the *Wave Inversion Technology (WIT) Consortium*.

REFERENCES

Forbriger, T., Groos, L., and Schäfer, M. (2014). Line-source simulation for shallow-seismic data. Part 1: Theoretical background. *Geophysical Journal International*, 198(3):1387–1404.

Groos, L., Schäfer, M., Forbriger, T., and Bohlen, T. (2017). Application of a complete workflow for 2D elastic full-waveform inversion to recorded shallow-seismic Rayleigh waves. *Geophysics*, 82(2):R109–R117.

Köhn, D., Meier, T., Fehr, M., Nil, D., and Auras, M. (2016). Application of 2D elastic Rayleigh waveform inversion to ultrasonic laboratory and field data. *Near Surface Geophysics*, 14(5):461–476.

Nuber, A., Manukyan, E., and Maurer, H. (2017). Optimizing measurement geometry for seismic near-surface full waveform inversion. *Geophysical Journal International*, 210(3):1909–1921.

Pan, Y., Xia, J., Xu, Y., Gao, L., and Xu, Z. (2016). Love-wave waveform inversion for shallow shear-wave velocity using a conjugate gradient algorithm. *Geophysics*, 81(1):R1–R14.

Pérez Solano, C., Donno, D., and Chauris, H. (2014). Alternative waveform inversion for surface wave analysis in 2-D media. *Geophysical Journal International*, 198(3):1359–1372.

Romdhane, A., Grandjean, G., Brossier, R., Rejiba, F., Operto, S., and Virieux, J. (2011). Shallow-structure characterization by 2D elastic full waveform inversion. *Geophysics*, 76(3):R81–R93.

Wittkamp, F. and Bohlen, T. (2016). Individual and joint 2-D elastic full waveform inversion of Rayleigh and Love waves. In *78th EAGE Conference and Exhibition 2016*.